

Wavelength Tunable Laser with Silica-Waveguide Ring Resonators

Takeshi TAKEUCHI^{†a)}, Morio TAKAHASHI[†], Kouichi SUZUKI^{††}, Members,
Shinya WATANABE^{††}, Nonmember, and Hiroyuki YAMAZAKI[†], Member

SUMMARY We have proposed a tunable laser with silica-waveguide ring resonators. In this tunable laser, a semiconductor optical amplifier was passively aligned and mounted onto a silica-waveguide substrate. The ring resonators can be tuned by controlling their temperatures using the thermo optic heaters formed on them, and there are no mechanically moving parts. Thus, they are sufficiently stable and reliable for practical use. Our tunable laser exhibits a high fiber-output power of more than 15 dBm and a wide tunable range of 60 nm (L-band, 50 GHz spacing, 147 channels). Moreover, a tunable laser with a much wider tunable range of 96 nm using 100-GHz-FSR ring resonators is also reported.

key words: tunable laser, photonic integrated circuit, silica-waveguide, ring resonator

1. Introduction

Wavelength tunable lasers have become key devices in optical network systems, such as wavelength division multiplexing (WDM) and reconfigurable optical add/drop multiplexing (ROADM) systems, where wavelength plays an important role. Using tunable lasers instead of conventional fixed wavelength lasers will significantly reduce the inventory cost for the light source. Moreover, tunable lasers make the optical network much more efficient and flexible. Several different device types have been proposed as tunable lasers; monolithic type lasers including a DFB-array type [1] and DBR type [2], [3], and external cavity lasers [4], [5]. In a monolithic type tunable laser, all fundamental functions are integrated on one chip. This makes the size of the tunable laser very compact, which is an advantage of a monolithic type laser. On the other hand, an external cavity laser is composed of a gain section and a tunable filter section. As a gain section, a semiconductor optical amplifier (SOA) is used in most of the cases. Device structure of an SOA chip is generally very simple and does not require complicated monolithic integration technology. This simplicity is an advantage of an external cavity laser.

The tunable laser we propose is also classified as an external cavity laser, composed of silica-waveguide ring resonators as a tunable filter section and a semiconductor optical amplifier (SOA) as a gain section [6]–[11]. The silica-

waveguide ring resonators and the SOA were automatically aligned and directly coupled using passive alignment technology [9]; thus, no complicated assembly procedures are required. The ring resonators can be tuned by controlling their temperatures using the thermo optic heaters formed on them, and there are no mechanically moving parts. Thus, they are sufficiently stable and reliable for practical use. Our fabricated tunable laser has exhibited a highly uniform high fiber output power of more than 15 dBm and a wide tunable range of 60 nm covering the full L-band. Also, a tunable laser with an enlarged tunable range up to 96 nm using 100-GHz-FSR ring resonators has been demonstrated.

2. Structure, Design, and Fabrication

2.1 Device Structure

The proposed tunable laser structure is schematically shown in Fig. 1. The tunable laser consists of a silica lightwave circuit and an SOA. As shown in Fig. 2, the SOA was mounted on the Si substrate of the silica lightwave circuit. The SOA and the lightwave circuit were directly butt-coupled using passive alignment technology, which will be described in detail in Sect. 2.4. The SOA was composed of a 1000- μm long gain section and a 280- μm long phase control section with a 220- μm long separation region between them. They had InP-based buried hetero structure waveguides with different compositional wavelength, and they were butt-jointed using regrowth technology. The phase control section is used to optimize the optical phase automatically by so-

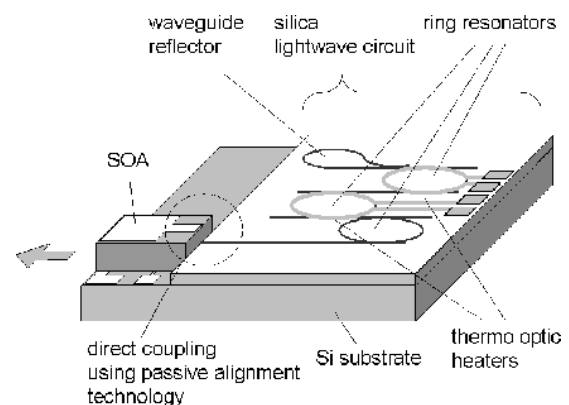


Fig. 1 Schematic of tunable laser.

Manuscript received June 2, 2008.

Manuscript revised October 16, 2008.

[†]The authors are with the Nano Electronics Research Laboratories, NEC Corp., Tsukuba-shi, 305-8501 Japan.

^{††}The authors are with the Fiber Optic Device Division, NEC Corp., Otsuki-shi, 401-0016 Japan.

a) E-mail: t-takeuchi@db.jp.nec.com

DOI: 10.1587/transele.E92.C.198

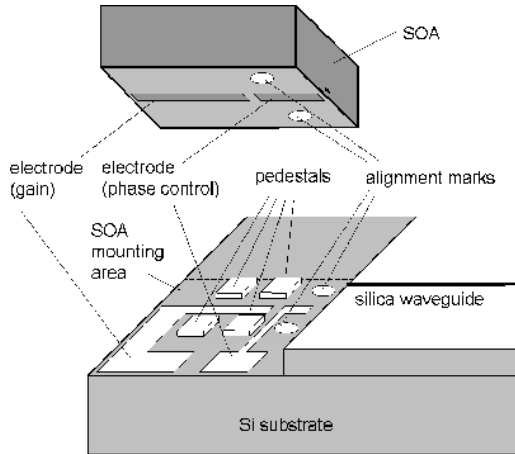


Fig. 2 Detailed structures around SOA.

called dither control system. In the dither control system, the phase current is modulated at a small amplitude. By monitoring the tapped optical output power, the DC component of the phase current is controlled so that the amplitude of the optical output power fluctuation caused by the modulation becomes smallest. Thus, the phase current is optimized to give the maximum optical output power. For this purpose, phase control section integrated in the SOA chip is suitable because of its sufficient response speed, while silica-waveguide based phase control section would be insufficient for 20-kHz modulation in our dither control system. The phase current modulation broadens the line width of the laser output, however, to suppress the stimulated Brillouin scattering, the adequately broadened line width is rather desirable. The lightwave circuit consists of three ring resonators which work as tunable filters by using the thermo optic heaters formed on the ring resonators. A waveguide reflector is also employed in the lightwave circuit as an external cavity mirror. Nitride-doped-silica (SiON) was used as the core material of the waveguides. The core was 2- μm wide and 1.4- μm thick, and it was embedded with silica. The refractive index contrast was 6%, which is large enough to suppress the excess loss at the bend waveguides of the lightwave circuit. Spot-size-converters were introduced in both the SOA and the lightwave circuit at the butt-coupling interface to enlarge the spot sizes on both sides and, consequently, to enlarge the coupling tolerance. The size of the tunable laser chip including both the SOA and the lightwave circuit was 6.5 mm long and 4.5 mm wide.

2.2 Wavelength Tuning Using Triple-Ring Resonators

Figure 3 shows the configuration of the silica lightwave circuit, and Fig. 4 shows the principle of wavelength tuning using the ring resonators. Three ring resonators, rings 1, 2, and 3, are cascaded in the lightwave circuit. Ring 1 has a free spectral range (FSR) of 50 GHz, which corresponds to the ITU-T grid spacing, and works as a wavelength reference ring. For the precise wavelength adjustment to the

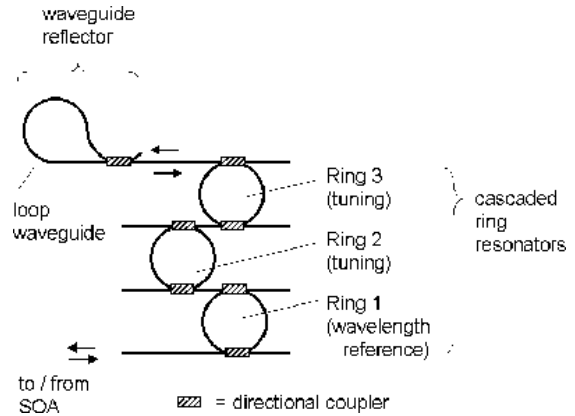


Fig. 3 Configuration of silica lightwave circuit.

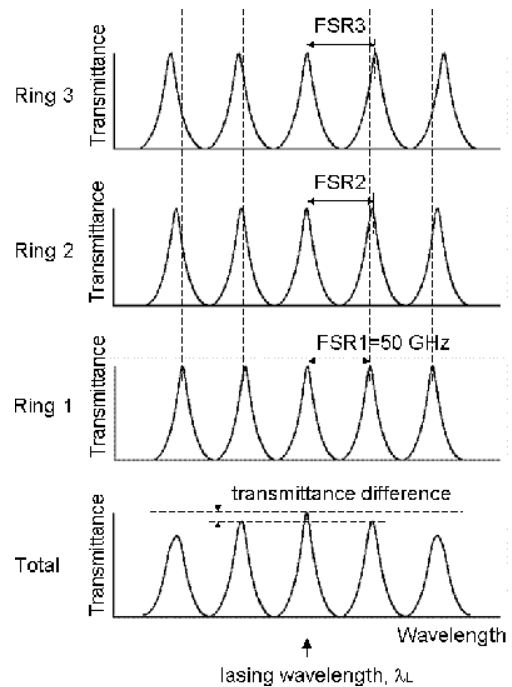


Fig. 4 Principle of wavelength tuning using three ring resonators.

ITU-T grid, the temperature of the ring 1 is controlled by the thermo optic heater. The FSRs of rings 2 and 3 (FSR 2, and FSR 3, respectively) are slightly larger than 50 GHz ($50 \text{ GHz} < \text{FSR } 2 < \text{FSR } 3$), as shown in Fig. 4. The total transmittance of the three rings, also shown in Fig. 4, has a maximum value at the wavelength of λ_L , where all the three rings have the maximum peak transmittance. The lasing occurs at this wavelength λ_L . We can select the lasing wavelength among the ITU-T channels by tuning the peak-transmittance wavelength of rings 2 and 3, which can be controlled with the thermo optic heaters. Although the tuning range of the peak-transmittance wavelength of each ring is not large enough, approximately 0.4 nm for the 200-mW power input to the thermo optic heater, the Vernier effect magnifies the tuning range of the lasing wavelength. The tuning range magnification factor M is determined by the equation $M =$

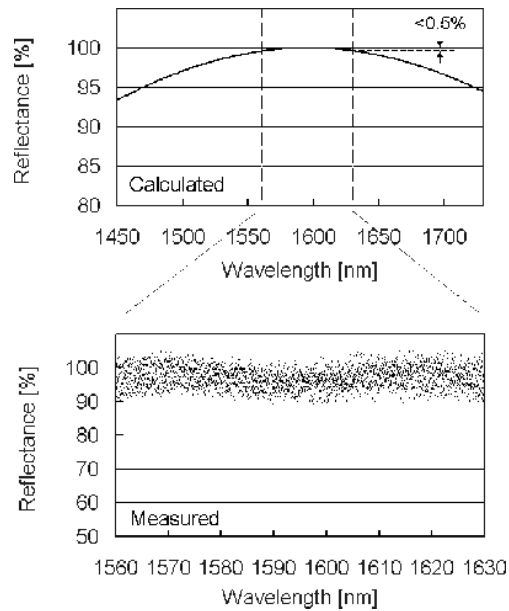


Fig. 5 Calculated and measured reflectance of waveguide reflector.

FSR 2/(FSR 2 – FSR 1), which means a smaller (FSR 2 – FSR 1) value gives a larger M . However, there is a design trade off, namely, a smaller (FSR 2 – FSR 1) value gives a smaller transmittance difference (threshold gain difference) between different channels (Fig. 4), and causes instability in lasing operations. The reason we have introduced the triple-ring structure is to relax this design trade off. The triple-ring structure gives a larger threshold gain difference compared with the double-ring structure which was previously reported [6], and provides a more stable lasing over a larger wavelength range.

2.3 Waveguide Reflector

As shown in Fig. 3, the waveguide reflector is a simple structure composed with a 3-dB directional coupler and a loop waveguide, which can be fabricated at the same process as the ring resonators. Thus, the fabrication cost is reduced using a waveguide reflector instead of a high reflection (HR) mirror used in previous works. Figure 5 shows calculated and measured reflectance of the waveguide reflector. A very flat and high reflectance of more than 95% has been confirmed over the L-band, which is in good agreement with the calculation. Here, the broadening of the measured reflectance value is due to Fabry-Perot interference caused by undesirable reflections inside the measurement system.

2.4 Passive Alignment Technology

As briefly described in Sect. 2.1, the SOA and the lightwave circuit were directly coupled using passive alignment technology [12], [13]. As shown in Fig. 2, a SOA-mounting area was formed on the silicon substrate of the lightwave circuit, where silica pedestals, alignment marks and electrodes were formed. The SOA chip was mounted with the junction-side

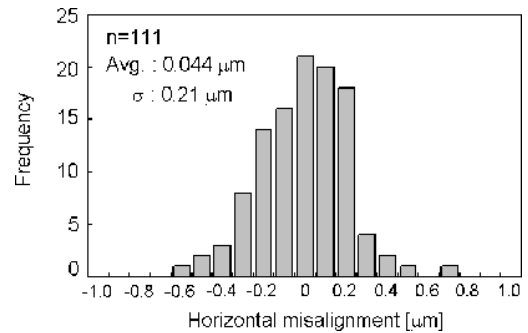


Fig. 6 Horizontal misalignment between SOA and lightwave circuit.

down. The vertical position of the SOA chip was precisely adjusted by the thickness of the silica pedestals. The vertical misalignment was less than $0.2 \mu\text{m}$, which was determined by the controllability of the silica-deposition thickness. Horizontal alignment was performed using the alignment marks, which were also formed on the SOA chip and can be observed with infrared light. Figure 6 shows a histogram of the horizontal misalignment between the SOA chip and the lightwave circuit. The average misalignment was $0.044 \mu\text{m}$, and the standard deviation was $0.21 \mu\text{m}$. The displacement of the SOA during the soldering process was successfully suppressed by optimizing the soldering conditions such as the thickness of the solder film and soldering temperature profiles. These values of vertical and horizontal misalignment are sufficiently small compared with coupling tolerance between the SOA and the silica waveguide. The 1-dB-down coupling tolerances (full width) were approximately $2 \mu\text{m}$ and $3 \mu\text{m}$ for vertical and horizontal direction, respectively. The average coupling loss between the SOA and the lightwave circuit was less than 1 dB.

3. Device Performance

Figure 7 shows the I-L characteristics of the fabricated tunable laser. No saturation was observed up to an injection current of more than 400 mA. A high fiber-coupled-output power of 15.5 dBm was obtained at a 300-mA injection current. The periodical power drops observed in the I-L curve were due to the optical phase mismatch in the laser cavity. As mentioned in Sect. 2.1, the optical phase will be always automatically controlled by the phase control section in the fully controlled operations, thus, no power drop will occur in practical use. A histogram of fiber-coupled optical output power is shown in Fig. 8. The average fiber-coupled output power was 15.5 dBm, and the standard deviation was 0.76 dBm. A high output power with high uniformity was achieved using passive alignment technology.

Figure 9 shows superimposed spectra of the tunable laser. The tunable range was 60 nm over the L-band, which contains 147 ITU-T channels with a channel-spacing of 50 GHz. Here, the longitudinal Fabry-Perot mode spacing was around 3 GHz. Only one longitudinal mode was chosen for lasing of each channel by adjusting the optical phase.

The fiber-coupled output power was more than 15 dBm at every channel. A lasing wavelength tuning map is shown in Fig. 10. A lattice like map suitable for wavelength control was obtained.

A butterfly module of the tunable laser is shown in Fig. 11. A tunable laser chip, which consisted of a silica lightwave circuit and an SOA mounted on it, was packaged with a thermo-electric cooler, a voltage-controlled optical attenuator, a monitor detector and an optical isolator. Here,

the optical attenuator was used to keep the SOA gain current constant and not to disturb the optical phase during the optical output power control. The package is compatible with conventional 14-pin packages with dimensions of $30 \times 12.7 \times 8.4 \text{ mm}^3$. A summary of the optical characteristics of the tunable laser module is shown in Fig. 12. The wavelength deviation was less than 6 pm from the ITU-T grid, the side-mode-suppression ratio was more than 51 dB,

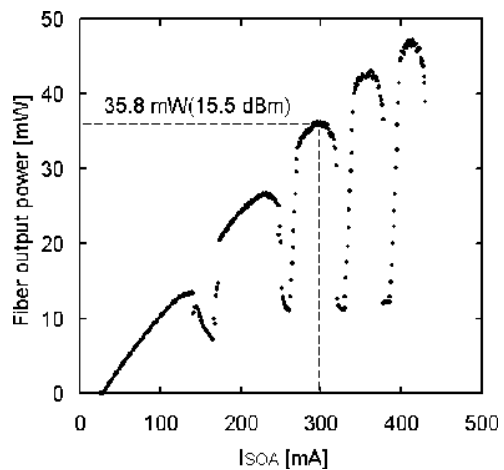


Fig. 7 I-L characteristics of tunable laser.

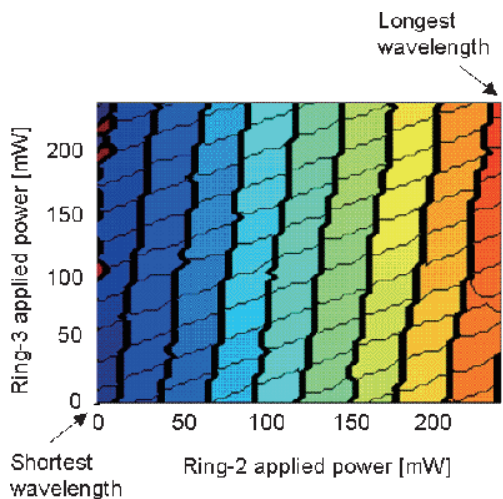


Fig. 10 Lasing wavelength tuning map.

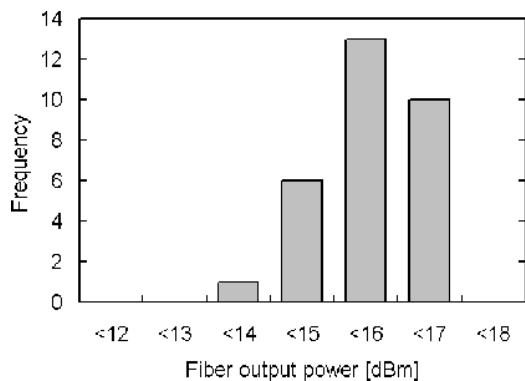


Fig. 8 Histogram of fiber coupled output power.

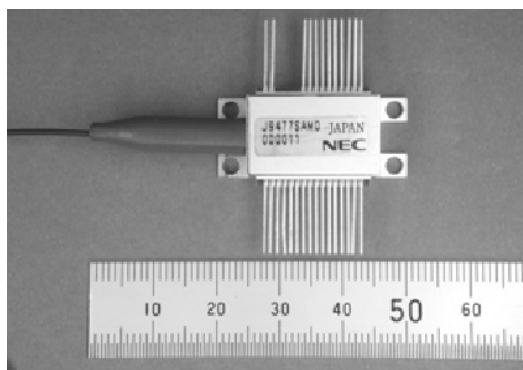


Fig. 11 14-pin butterfly package of tunable laser.

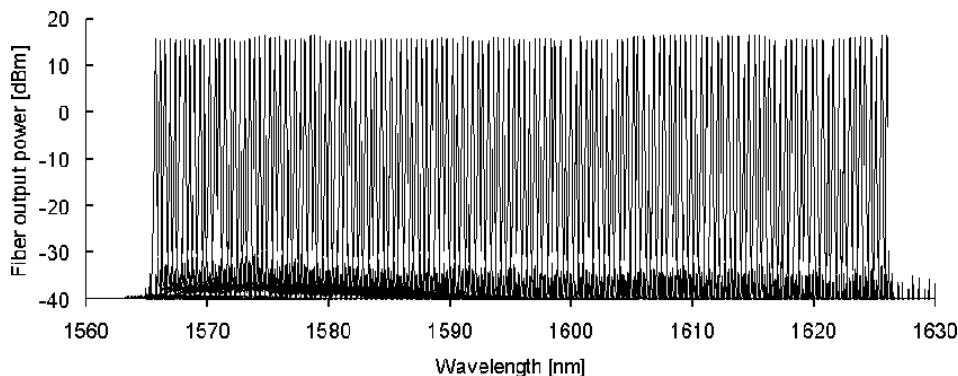


Fig. 9 Superimposed spectra of tunable laser with 50-GHz-ring resonators.

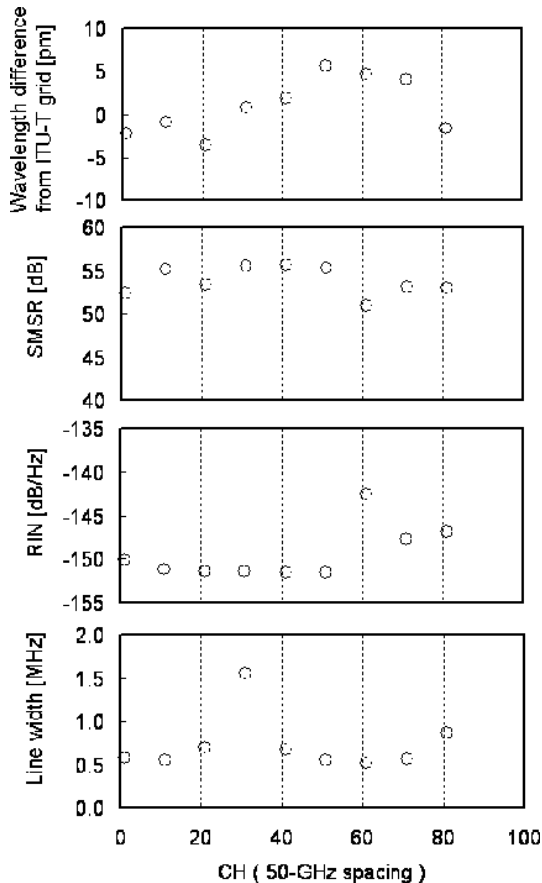


Fig. 12 Measured characteristics of tunable laser module.

the relative intensity noise (RIN) was less than -143 dB/Hz. Spectral line widths at most of the channels were between 0.5 MHz and 1 MHz. Only one channel exhibited a relatively large line width value of 1.6 MHz, which is thought to be affected by some electric noise introduced into the SOA gain current. Still, obtained characteristics are sufficient for practical use.

4. Widely Tunable Laser with 100-GHz-FSR Ring Resonators

As described in Sect. 2.2, there is a design trade off between a tunable wavelength range and a threshold gain difference. A threshold gain difference is an important factor which determines the stability of single-mode lasing without grid hopping. One solution for the trade off is to use the triple ring structure instead of the double ring structure, as previously mentioned in Sect. 2.2. Here, we report on another solution for the trade off, namely, the use of ring resonators with 100-GHz FSR instead of 50-GHz FSR. In Sect. 2.2, an equation is described for the tunable range magnification factor, $M = \text{FSR } 2 / (\text{FSR } 2 - \text{FSR } 1)$. This equation also gives a rough explanation of why the use of 100-GHz-rings solves the design trade off. From this equation, we can derive the second equation, $(M \times \text{FSR } 1) = (\text{FSR } 1 \times \text{FSR } 2) / (\text{FSR } 1 - \text{FSR } 2)$. Here, $(M \times \text{FSR } 1)$ is the tun-

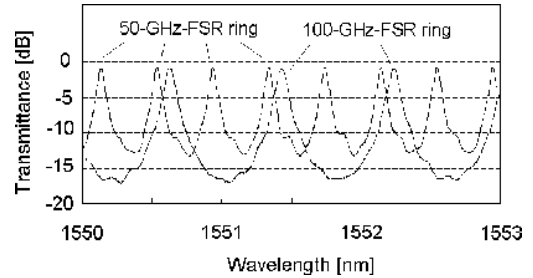


Fig. 13 Transmittance spectra of 50-GHz and 100-GHz FSR single ring.

able wavelength range, and the $(\text{FSR } 2 - \text{FSR } 1)$ value determines the transmittance difference (threshold gain difference). Namely, the second equation is a trade-off equation between the tunable wavelength range and the gain difference. Using the ring resonators with large FSR values gives a large $(\text{FSR } 1 \times \text{FSR } 2)$ value. According to the trade off equation, a larger $(\text{FSR } 1 \times \text{FSR } 2)$ value gives a larger $(M \times \text{FSR } 1)$ value for the same $(\text{FSR } 1 - \text{FSR } 2)$ value (which means a larger tunable range for the same gain difference), or gives a larger $(\text{FSR } 1 - \text{FSR } 2)$ value for the same $(M \times \text{FSR } 1)$ value (which means a larger gain difference for the same tunable range). Thus, the trade off between the tunable range and the gain difference can be relaxed using larger FSR rings such as 100-GHz rings.

The radius of a 100-GHz-FSR ring is $280 \mu\text{m}$, which is half the radius of a 50-GHz-FSR ring. In general, a bend waveguide with a smaller curvature radius has a higher excess loss. However, because of the large refractive index contrast of 6% in our SiON-core waveguide, the excess loss was sufficiently suppressed even in the 100-GHz-FSR rings. Figure 13 shows transmittance spectra of single ring resonators with 50-GHz FSR and 100-GHz FSR. The transmittance losses for the 50-GHz and 100-GHz rings were almost the same and small enough for the device application. The compactness of the 100-GHz ring is also an advantage from the viewpoint of mass production. The area of the 100-GHz ring is only 25% that of the 50-GHz ring, thus, the device yield of the silica lightwave circuit chips per wafer becomes much higher when 100-GHz rings are used.

We fabricated a tunable laser with 100-GHz-FSR triple ring resonators. The basic structure of the laser is the same as described in Sect. 2.1. The first ring resonator has a FSR of 100 GHz, which works as a wavelength reference ring. By switching the π -shift power ON and OFF at the thermo optic heater, the 100-GHz reference ring provides the ITU-T grid with a 50-GHz spacing. The second and the third ring resonators have FSRs that are slightly smaller than 100 GHz. They work as tuning rings using the Vernier effect. The FSRs of the tuning rings determine the theoretical value of the tunable wavelength range of the ring resonators, which was designed to be 95 nm in the fabricated device. The ring-resonator chip size was $2.5 \times 3.0 \text{ mm}^2$.

Figure 14 shows superimposed spectra of the fabricated tunable laser. The lasing wavelength range was from 1540 to 1636 nm. The measured tunable range of 96 nm was in good

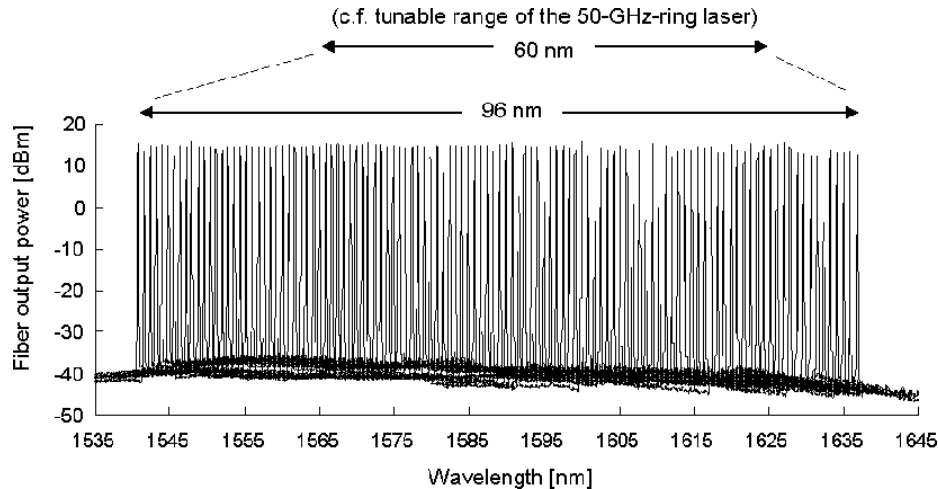


Fig. 14 Superimposed spectra of tunable laser with 100-GHz-FSR ring resonators.

agreement with the designed tunable range of 95 nm. In this measurement, the channel spacing was 100 GHz; however, a 50-GHz spacing could be obtained with a π -shift power being applied to the thermo optic heater of the reference ring. The fiber output power was more than 13 dBm, and the side-mode-suppression ratio was more than 50 dB throughout the whole tuning range. Stable single-mode lasing over a large wavelength region was obtained, which proves the high potential of the widely tunable laser with 100-GHz-FSR ring resonators for practical use.

5. Conclusion

We have proposed a tunable laser with silica-waveguide ring resonators. The proposed laser has a simple structure, which is suitable for mass production. The tunable laser exhibits a high fiber-output power of more than 15 dBm and a wide tunable range of 60 nm (L-band, 50-GHz spacing, 147ch). Moreover, a tunable laser with a much wider tunable range of 96 nm with 100-GHz-FSR ring resonators has also been reported.

References

- [1] K. Yashiki, K. Sato, T. Morimoto, S. Sudo, K. Naniwae, S. Ae, K. Shiba, N. Suzuki, T. Sasaki, and K. Kudo, "Wavelength-selectable light sources fabricated using advanced microarray-selective epitaxy," *IEEE Photonics Technol. Lett.*, vol.16, no.7, pp.1619–1621, July 2004.
- [2] Y.A. Akulova, G.A. Fish, P.C. Koh, C.L. Schow, P. Kozodoy, A.P. Dahl, S. Nakagawa, M.C. Larson, M.P. Mack, T.A. Strand, C.W. Coldren, E. Hegblom, S.K. Penniman, T. Wipiejewski, and L.A. Coldren, "Widely tunable electroabsorption-modulated sampled-grating DBR laser transmitter," *IEEE J. Sel. Top. Quantum Electron.*, vol.8, no.6, pp.1349–1357, Nov./Dec. 2002.
- [3] D.J. Robbins, G Busico, L. Ponnampalam, J.P. Duck, P.J. Williams, R.A. Griffin, A.J. Ward, D.C.J. Reid, N.D. Whitbread, and E. Barton, "A high power, broadband tunable laser module based on a DS-DBR laser with integrated SOA," *Tech. Dig. Optical Fiber Communication Conference (OFC)*, no.TuE3, California, USA, Feb. 2004.
- [4] D. Anthon, J.D. Berger, and A. Tselikov, "C+L band MEMS tunable external cavity semiconductor laser," *Tech. Dig. Optical Fiber Communication Conference (OFC)*, no.WL2, California, USA, Feb. 2004.
- [5] J. De Merlier, K. Mizutani, S. Sudo, K. Naniwae, Y. Furushima, S. Sato, K. Sato, and K. Kudo, "Full C-band external cavity wavelength tunable laser using a liquid-crystal-based tunable mirror," *IEEE Photonics Technol. Lett.*, vol.17, no.3, pp.681–683, July 2005.
- [6] H. Yamazaki, M. Ishizaka, M. Takahashi, S. Watanabe, K. Suzuki, K. Sato, and S. Sudo, "Widely tunable laser consisting of a silica waveguide double ring resonator connected directly to a semiconductor optical amplifier," *Proc. 30th European Conf. on Opt. Commun.*, post-deadline paper no.4-2-4, Stockholm, Sweden, Sept. 2004.
- [7] M. Takahashi, Y. Deki, S. Takaesu, M. Horie, M. Ishizaka, K. Sato, K. Kudo, K. Suzuki, T. Kaneko, X. Xu, and H. Yamazaki, "A stable widely tunable laser using a silica-waveguide triple-ring resonator," *Optical Fiber Communication Conference (OFC)*, postdeadline paper PDP19, California USA, March 2005.
- [8] Y. Deki, M. Takahashi, K. Suzuki, M. Ishizaka, S. Takaesu, M. Horie, K. Sato, K. Kudo, and H. Yamazaki, "A 160-nm-wavelength tunable laser using a waveguide double-ring resonator," *Proc. 31st European Conf. on Opt. Commun.*, no.7F3-3, Glasgow, UK, Sept. 2005.
- [9] S. Watanabe, M. Takahashi, K. Suzuki, T. Takeuchi, Y. Deki, T. Hatanaka, N. Sakuma, A. Kawachi, S. Takaesu, M. Horie, T. Miyazaki, M. Kurihara, M. Kanemoto, T. Kaneko, I. Tomita, M. Namiwaka, M. Nido, and H. Yamazaki, "High power tunable resonated-ring-reflector laser using passive alignment technology," *Proc. 32nd European Conf. on Opt. Commun.*, no.Tu3.4.6, Cannes, France, Sept. 2006.
- [10] Y. Deki, T. Hatanaka, M. Takahashi, T. Takeuchi, S. Watanabe, S. Takaesu, T. Miyazaki, M. Horie, and H. Yamazaki, "Wide-wavelength tunable lasers with 100 GHz FSR ring resonators," *Electron. Lett.*, vol.43, no.4, pp.225–226, Feb. 2007.
- [11] R. Todt, S. Watanabe, Y. Deki, M. Takahashi, T. Takeuchi, S. Takaesu, T. Miyazaki, M. Horie, and H. Yamazaki, "Widely tunable resonated-ring-reflector lasers covering C- and L-bands," *Proc. 33rd European Conf. on Opt. Commun.*, no.PD2.5, Berlin, Germany, Sept. 2007.
- [12] K. Kurata, K. Yamauchi, A. Kawatani, H. Tanaka, H. Honmou, and S. Ishikawa, "A surface mount type single-mode laser module using passive alignment," *Trans. Compon. Packag. Manuf. Technol. Part B*, vol.19, no.3, pp.524–531, 1995.
- [13] K. Kurata, "Mass production techniques for optical modules," *Proc. 48th Electronic Components and Technology Conference*, pp.572–580, 1998.



Takeshi Takeuchi received his B.E. and M.E. degrees in physical electronics engineering from the Tokyo Institute of Technology in 1988 and 1990, respectively. Since he joined NEC Corporation in 1990, he has been engaged in the research and development of opto-electronic devices such as photo detectors and photonic integrated circuits. In 2005, he started his work on tunable lasers.



Morio Takahashi received his Ph.D. degree from Tokyo University of Agriculture and Technology in 2001. Since he joined NEC Corporation in 2001, he has been engaged in the research and development of opto-electronic devices.



Kouichi Suzuki received his B.E., M.E. and Ph.D. degrees in electronics and applied physics from the Tokyo Institute of Technology, in 1995, 1997 and 2000, Tokyo, Japan, respectively. Since he joined NEC Corporation in 2000, he has been engaged in the research and development of opto-electronic devices such as planar lightwave circuits for optical communication systems. In 2004, he started his work on tunable lasers.



Shinya Watanabe received his B.E. and M.E. degrees in electronic engineering from Niigata University in 1995 and 1997, respectively. Since he joined NEC Corporation in 1997, he has been engaged in the research and development of processes for the waveguides circuits. In 2004, he started his work on tunable lasers.



Hiroyuki Yamazaki was born in Hokkaido, Japan, on March 13, 1964. He received the B.E. and M.E. degrees in electrical engineering from Tokai University, Kanagawa, Japan, in 1986 and 1988, and Ph.D. degrees in electronics and applied physics from the Tokyo Institute of Technology, in 2007, Tokyo, Japan, respectively. Since 1988, he has been with the Opto-electronics Research Laboratories, NEC Corporation, where he was engaged in research and development on semiconductor lasers and optical

passive devices for optical communications.